Manuscript Click here to download Manuscript Spensley_Fraser.pdf

Acute effects of drugs on *C.elegans* movement reveal complex responses and plasticity

Diversity of Acute Drug Responses in C. elegans

Mark Spensley[1], Samantha Del Borrello[1,2], Djina Pajkic[1] and Andrew G Fraser[1,2]

[1] Donnelly Centre for Cellular and Biomolecular Research, University of Toronto, Toronto, Ontario, Canada

[2] Department of Molecular Genetics, University of Toronto, Toronto, Ontario, Canada

Abstract

Many drugs act very rapidly — they can turn on or off their targets within minutes in a whole animal. What are the acute effects of drug treatment and how does an animal respond to these? We developed a simple assay to measure the acute effects of drugs on *C.elegans* movement and examined the effects of a range of compounds including neuroactive drugs, toxins, environmental stresses and novel compounds on worm movement over a time period of 3 hours. We find that many treatments show complex acute responses — a phase of rapid paralysis is followed by one or more recovery phases. The recoveries are not the result of some generic stress response but are specific to the drug e.g. recovery from paralysis due to a neuroactive drug requires neurotransmitter pathways whereas recovery from a metabolic inhibitor requires metabolic changes. Finally, we also find that acute responses can vary greatly across development and that there is extensive and complex natural variation in acute responses. In summary, acute responses are sensitive probes of the ability of biological networks to respond to drug treatment and these responses can reveal the action of unexplored pathways.

Author Summary

Drugs are powerful tools that let us switch on or off key pathways in whole animals and watch the effects. Here we set up a simple assay to measure how drugs affect the movement of the simple nematode *C.elegans* — crucially, we look how those responses

change over time. We find that worms have complex responses to many different drugs — they go through clear phases of paralysis and recovery. The recovery from the initial effect of any drug is not due to a generic stress response but is specific to the way each drug acts. We find for example that worms can recover from paralysis driven by one neurotransmitter pathway by activating a different neurotransmitter pathway or from paralysis caused by loss of one metabolic pathway by turning on a second one. These complex responses show how the basic genetic networks that are needed for normal behaviour and function can rewire and respond to the effect of many drugs. Importantly, the responses can vary in many ways — different aged worms or different individuals can have different responses and capturing how drug responses change over time is critical to dissect this complexity.

Introduction

Drugs are extremely powerful research tools. Addition of a drug can turn on or off a specific target protein and the effect on the organism can be followed over time. In model organisms, a well-characterized drug response can form the basis for genetic screens to identify the drug target and to find genes that modulate the effect of the drug. In *C.elegans*, for example, genetic screens for mutants with altered drug responses were key to finding the targets of several major anthelmintics (1–4) as well as to identifying core components of conserved neuronal signaling pathways (5,1,6,7).

Many genetic screens for *C.elegans* mutants with altered drug responses have screened for mutants that escape the effects of chronic exposure to drugs. In these screens, populations of mutant worms are typically exposed to drugs for several days (8–13). However, many drugs act very rapidly on worms yet currently relatively little is known about these acute responses of *C.elegans* to drugs. What do acute responses generally look like? Are acute responses the same at all developmental stages? Is there natural variation in acute responses as there is in mutant phenotypes or chronic drug responses? Do multiple drugs with the same long-term effect have the same acute responses or very different ones? What are the genes that affect the acute responses — are they the same or different genes as those that affect long-term drug effects?

Our goal in this study was to examine acute drug responses in *C.elegans* and address at least some of these questions. We developed an image-based method that accurately measures worm movement at high throughput. This allows us to gather

69 rich information about the acute effects of drugs on worm movement, measuring
70 both the effect of a range of doses of drugs and how the effects of any drug changes
71 across time. We examined a wide range of drugs that were previously shown to be
72 bioactive as well as a number of environmental stresses. We found that many drugs
73 have complex acute effects on worms indicating that the animal responds rapidly to
74 the initial drug effect — these acute responses include both transient and sustained
75 recovery from initial paralysis. We show that the basis for complex acute responses
76 is drug-specific and that acute responses can differ greatly between different
77 developmental stages. Finally, we compare acute responses in two isolates and find
78 that there is substantial variation in acute responses and that this changes with
79 dose, time and developmental stage. We thus find that measuring acute responses to
80 drugs can reveal the action of unexplored pathways and that acute responses vary
81 extensively and at many levels between different individuals. The ability to measure
82 acute responses at high throughput will allow both drug screens and genetic screens
83 to uncover the underlying molecular basis for these complex responses.

84

85 # Results

86 ## Development of a high throughput image-based movement assay

87 We wanted to measure the acute effects of drugs on worms over the time period of
88 minutes to hours. We focused on movement as a key phenotype — a very wide
89 range of compounds affect movement including toxins, neuroactive compounds and
90 environmental stresses. There are a wide variety of assays to measure the acute

91 effects of drugs on worm movement, with different levels of throughput and
92 resolution, and different requirements for specialized equipment such as worm
93 trackers or microfluidic devices (14–19). Here we focused on creating a simple
94 assay for worm movement that allows us to follow how worms respond to drug
95 treatment over time periods ranging from minutes to hours. The assay is simple,
96 automated, gives quantitative data and has sufficient throughput to efficiently
97 analyse responses to thousands of drugs.

98 In outline, our assay measures the movement of worms in 96-well format in liquid.
99 Worms are continuously bathed in buffer containing the compound and there are
100 multiple worms in each well (e.g. ~100 L1 larvae). We capture two successive
101 images of each well, separated by a 500 millisecond interval — by comparing these
102 two images we identify the extent of worm movement at any particular time point
103 or drug concentration (see Fig 1A for details) and calculate a fractional mobility
104 score (FMS) for each well at any individual time point. Worm movement can be
105 measured at many time points to provide a time-course of the effect of a given drug
106 concentration on worm movement (Fig 1B, right), at a range of drug concentrations
107 to yield a dose-response curve (Fig 1B, lower) or (since the throughput is high
108 enough) to cover both dose and time responses. The assay can thus be used to give a
109 rich quantitative measurement of the effect of any drug on worm movement.

110 To validate our assay, and in particular to ensure that detected effects on movement
111 are specific to the targeted pathway, we examined the response of adult worms to
112 aldicarb (Ald), a very well characterised neuro-active compound (reviewed in depth
113 in (20)). Acetylcholine (ACh) is a core neurotransmitter that is critical for normal

114 movement (21). Following release of ACh at synapses, ACh is rapidly metabolised by
115 acetylcholinesterases to turn off ACh responses. Aldicarb is a carbamate
116 acetylcholinesterase inhibitor — Ald thus increases the local concentration of ACh at
117 the synapse or neuromuscular junction by reducing the rate of degradation of
118 endogenous released ACh (22). Aldi is known to cause paralysis in *C. elegans*, via the
119 sustained activation of ionotropic acetylcholine receptors (nAChRs) and ACh
120 signalling and the effects of both Ald and ACh have been extremely well studied
121 (reviewed in (20)). We thus wanted to validate our assay by testing whether we can
122 detect the well-established effects of Ald to induce paralysis and whether any Ald-
123 induced paralysis is mediated by the well-characterised nAChR subunits, confirming
124 that the effects we see are specific.

125 Consistent with previous studies, we found that Ald treatment results in paralysis of
126 adult worms. Both the extent of paralysis and the rate of onset were dose dependent
127 (Fig 2A). Aldicarb-induced paralysis is mediated by activation of nAChRs in body
128 wall muscles; nAChRs are ligand gated ion channels composed of five subunits (23–
129 26). Several of these subunits are known to be required for ACh-driven paralysis
130 including UNC-38, UNC-63 and LEV-8. (23–25) To confirm that the effects of drugs
131 on movement that we detect in our assay are specific to the activation of known
132 AChRs (and not due to some kind of non-specific toxicity for example), we tested the
133 response of mutant worms lacking functional copies of each of these subunits. As
134 expected from previous studies, adult worms homozygous for loss-of-function
135 mutations in *unc-38*, *unc-63*, *lev-8*, *lev-1* or *unc-29* are markedly less sensitive (Fig
136 2B, Fig S1). We also find that mecamylamine, a non-competitive nAChR antagonist,

137 affects the dose-response relationship of aldicarb: in the presence of 600 μM
138 mecamylamine, the EC50 of aldicarb shifts from 0.76 mM to 1.6 mM, with a slight
139 decrease in maximal response (Fig 2C). The effects of Ald on worm movement that
140 we measure in our assay are thus specific to the action of elevated ACh on nAChRs
141 and not some non-specific effect on movement.

142 We note that while we focus here on the use of this assay to measure the effects of
143 drugs on worm movement, it can also be used to measure the effect of genetic
144 perturbations on movement directly. To illustrate this, we used RNA-mediated
145 interference (RNAi) to knock down 7 genes that are known to be required for wild-
146 type movement and measured movement after RNAi. We found robust RNAi
147 phenotypes for all 7 genes (Fig 2D) showing that our movement assay is applicable
148 to both genetic and drug based screens. Thus, we expect our method to be
149 applicable in a range of pharmacological, genetic, and RNAi experiments.

150 We have thus developed a simple method that allows us to measure the acute effects
151 of drug treatments on worm movement at high throughput. We showed that our
152 assay recapitulates the known effects of the well-characterised neuroactive drug Ald
153 and that this is indeed due to its known mode of action through the activation of
154 specific receptors. Crucially, our assay allows us to measure both dose responses
155 and time-resolved responses to drugs. In the rest of this paper we demonstrate that
156 time-resolved profiles of drug responses can yield new insights into *C. elegans*
157 biology.

158 ## Acute responses to drugs are often complex

159 We established a simple assay to measure acute responses of worms to drugs over
160 time periods of minutes to hours. We wanted first to use this to explore acute
161 responses in general — what do these look like for a variety of drugs and
162 treatments? We exposed *C.elegans* L1 larvae to a wide range of different compounds
163 and treatments including compounds that inhibit core essential machineries such as
164 the electron transport chain (inhibition by potassium cyanide, KCN, shown in Fig
165 3A) or the ribosome (effect of cycloheximide in Fig 3B), environmental stresses such
166 as high salt conditions (NaCl shown in Fig 3C), known nematicides (abamectin
167 shown in Fig 3D), as well as compounds that affect movement via altered
168 neurotransmission (e.g. aldicarb Fig 2A). In each case, worms were treated and their
169 movement examined over a time course of 3 hours — at least 3 biological replicates
170 were done for each treatment.

171 In addition to this panel of characterized compounds, we also tested a range of novel
172 compounds that had been identified as affecting worm growth in chronic exposure,
173 population growth assays (13). We examined the effects of 170 of these on the
174 movement of L1 larvae and find that many (53/170) also have acute effects on
175 worm movement. Crucially, an unexpectedly high proportion (31 of 53 with acute
176 effects; 58%) of drugs tested show complex time-resolved responses illustrated in
177 Fig 3E-G, including either sustained or transient recovery from initial drug effects.

178 Having looked at acute responses to across a range of different treatments, we found
179 complex acute responses across every type of compound, including neuro-active

180 compounds, environmental stresses, and toxins that target essential genes. These
181 responses can be very complex — for example, the novel compound shown in Fig 3G
182 has two distinct phases of recovery and several structurally related compounds
183 have similarly complex responses (data not shown). We note that every one of these
184 complex drug responses can be the basis either for a genetic screen for mutants
185 with altered responses or for drug screens for compounds that modulate the
186 response. This complexity of many acute drug responses underlines the need to be
187 able to measure time-resolved acute effects of drugs on movement.

188 The complex effects of many compounds over time suggest that the worms are
189 responding to many drug treatments in some way — for example, several drugs
190 cause an initial rapid paralysis followed by a recovery phase where the worms begin
191 to move again at almost normal rates. What underlies this recovery? Is it some
192 generic stress or xenobiotic response or does the worm respond in specific ways to
193 each compound? To gain some insights into this we focused on the acute responses
194 to two well-characterized compounds, Aldicarb and cyanide.

195 Agonists of acetylcholine signalling have complex effects on worm movement 196 that change across development

197 As shown in Fig 2A treatment of adult animals with Ald results in a rapid reduction
198 in movement and sustained paralysis. Interestingly, we found that L1 animals
199 behave completely differently— Ald induces rapid paralysis of L1 worms but this is
200 followed by a more gradual recovery (Fig 4A; S2). To further examine the Ald
201 response across development, we tested all developmental stages and found the

202 response is qualitatively very different across development (Fig 4A). L1 and L2
203 stage larvae show an initial phase where Ald treatment results in reduced
204 movement, followed by a recovery phase during which paralysis is gradually
205 relieved. As worms progress through the four larval stages, the initial paralysis
206 remains similar but this recovery is reduced, becoming minimal by adulthood. What
207 underlies this recovery in L1 and L2 animals?

208 To further explor the recovery of L1s from paralysis, we asked whether this is
209 specific to Ald or whether other drugs that affect ACh signaling show similar acute
210 responses. Ald affects ACh signalling by preventing the degradation of ACh — it does
211 not activate ACh receptors directly nor does its action have any specificity for any
212 specific sub-type of ACh receptor. Nicotine (Nic) activates ACh signaling in a
213 different way — it is a direct agonist of specific ACh receptors, the nicotinic ligand-
214 gated ion channels. We compared their acute responses and find that both Ald and
215 Nic show a rapid initial paralysis followed by a recovery of movement (Fig 4B).
216 While these two responses have superficial similarities, there is a crucial difference
217 in the recovery phase. For Nic, while L1 worms recover from the reduction of
218 movement caused by low doses of Nic, increasing concentrations of Nic result in
219 greater paralysis and less recovery until at high Nic doses there is no appreciable
220 recovery (Fig 4D). For Ald, we see the precise opposite — there is no recovery at
221 low doses of Ald, but recovery increases with increasing Ald (Fig 4C). This suggests
222 that the recovery from Ald and Nic-induced paralysis is fundamentally different and
223 that Ald is somehow driving recovery since the more Ald we add, the stronger the
224 recovery. How could Ald be acting and how could this be different to Nic?

225 ACh is known to activate two completely different classes of receptor: ligand-gated
226 ion channels (nAChRs) and muscarinic ACh receptors (mAChRs). nAChRs act rapidly
227 and are stimulated directly by Nic and indirectly by Ald via its action to increase
228 ACh. mAChRs have much more complex G-protein coupled signaling — crucially,
229 they are not activated by Nic but are also activated following Ald treatment. We
230 hypothesized that the Ald recovery phase might be mediated by mAChRs and test
231 this below.

232

233 Recovery from rapid paralysis induced by Aldicarb occurs via muscarinic receptor 234 signaling

235 To test whether recovery from Ald-induced paralysis might be due to the activation
236 of mAChRs, we examined whether a mAChR antagonist, atropine (Atr), could block
237 the recovery phase of the Ald response. This is indeed the case (Fig 5A) suggesting
238 that recovery is the result of an activation of mAChR signaling following increased
239 ACh levels after Ald treatment. The *C. elegans* genome encodes three muscarinic
240 acetylcholine receptors, GAR-1, GAR-2 and GAR-3 (27–29) — we obtained deletion
241 mutants for each of these receptors and tested whether the effect Ald was altered in
242 these mutant strains. The Ald response is clearly different in the *gar-3(gk305)*
243 mutant strain: while the paralysis phase appears very similar to wild-type, the
244 recovery phase is strongly suppressed in the *gar-3(gk305)* mutant, although not
245 completely abolished (Fig 5B). We note that mutations in *gar-1* and *gar-2* also have

246 effects on recovery but these are much weaker and we suggest that *gar-3* is the key
247 mAChR that drives recovery from nAChR stimulation in L1 animals.

248 We thus propose that Ald causes a complex acute response in L1 worms because the
249 increased ACh levels have effects on two separate neurosignalling pathways. The
250 first phase of the acute response is a rapid reduction in movement due to activation
251 of nAChRs. The second phase is a slower recovery due to activation of mAChRs
252 which somehow relieve the nAChR-driven paralysis. To further test this, we
253 examined whether we can drive recovery from Nic-induced paralysis with agonists
254 of mAChRs. Nic can only stimulate nAChRs and has no activity on mAChRs (30).
255 Consistent with our model, we find that we can induce recovery from Nic-induced
256 paralysis either by adding Ald (Fig 5C) or the mAChR agonists, Oxotremorine M
257 (OxoM) or Arecoline (Are) (Fig 5D; supplementary S3). To confirm that the same
258 mAChR requirement apply to OxoM-induced recovery as in Ald responses, we tested
259 the ability of each *gar* mutant to recover from Nic-induced paralysis in the presence
260 of OxoM (Fig 5E). We found that *gar-3* is indeed the primary mAChR driving OxoM-
261 induced recovery. Our data suggest that mAChR signalling can drive recovery from
262 paralysis induced by sustained nAChR activation. Finally, we examined whether
263 changes in mAChR signalling might underlie the difference in the ability of L1 and
264 adults to recover from Ald paralysis. We find that stimulation of mAChR signalling
265 by OxoM in adults cannot override the paralysis response (Fig 5F) and thus, changes
266 in the mAChR signalling machinery might indeed account for the different responses
267 across development.

268 Our data thus suggest that a model in which there is some kind of physiological
269 cross talk between two types of ACh receptor, nAChRs and mAChRs. This model is
270 summarized in Fig 6, and suggests that i) sustained activation of nAChRs alone
271 results in long-term paralysis, ii) sustained activation of mAChRs alone has little
272 effect on movement, but iii) dual activation of both nAChRs and the mAChR GAR-3,
273 such as with Ald alone, or Nic + OxoM results in an initial phase of nAChR-driven
274 paralysis followed by a slower mAChR-driven recovery. We conclude that the
275 complex acute response of L1 worms to Ald is highly specific to the drug used and is
276 not a generic stress or xenobiotic response. To examine whether this is true for
277 other drugs, we next looked at the effects of a very different drug, KCN, on worm
278 movement.

279

280 ### *C.elegans* has a complex response to treatment with cyanide.

281 Cyanide (KCN from here on) has a very well-characterized mode of action: it inhibits
282 aerobic metabolism by blocking the mitochondrial electron transport chain (ETC)
283 through binding to complex IV (reviewed in (31)). KCN is toxic to *C.elegans*
284 following prolonged exposure — here we examined the acute responses of worms
285 to KCN exposure.

286 We immediately noticed that the dose response at early time points were very
287 unusual — while intermediate doses of KCN caused almost complete paralysis
288 movement, high doses appeared to have little effect (Fig 7A). This was most

289 pronounced in DRCs between 15-30minutes — by ~60 minutes the DRCs appeared
290 much more normal, with increased effects being seen with increased dose.

291 How can the effect of low concentrations of KCN be greater than the effect of high
292 concentrations? We reasoned that this may be due to rewiring of metabolic
293 pathways — worms might respond to high KCN concentrations by rapidly switching
294 to use alternative metabolic pathways for generating ATP. An obvious candidate for
295 such a pathway was anaerobic glycolysis which is the major pathway for ATP
296 generation in anaerobic conditions in many animals — indeed we found that
297 addition of 2-deoxy-D-glucose, an inhibitor of phosphoglucose isomerase, a critical
298 enzyme in anaerobic glycolysis, caused a profound change in KCN DRCs. Worms can
299 no longer continue moving in high doses of KCN when 2DG is also present — instead
300 we find that increased concentrations of KCN result in decreased movement at all
301 time points (Fig 7A). This suggests that the unusual DRCs seen for KCN alone were
302 due to a shift to utilization of anaerobic glycolysis at early timepoints in high KCN
303 (Fig 7B).

304 This underscores the importance of measuring drug responses across time — if we
305 had only measured KCN DRCs at 80 minutes, they would have looked completely
306 unremarkable. It also confirms that the way that worms respond to acute drug
307 treatment is highly specific to the drug itself — while the aldicarb response involves
308 crosstalk between nAChRs and mAChRs, the KCN response involves metabolic
309 switches. The rapid responses of worms to compounds thus do not appear to be
310 generic stress or xenobiotic responses but are specific responses to the specific drug

311 effects. They reveal how the organism can rewire and adapt to sudden inhibition of
312 a key pathway.

313

314 Natural variation in acute drug response is very complex

315 Drug responses are known to vary within natural populations. In *C.elegans*, natural
316 variation in drug responses has been seen for several drugs including abamectin
317 and etoposide (32,33). In a previous study we compared the effects of KCN on two
318 natural isolates, the N2 and CB4856 isolate (34). These differ by around
319 1SNP/800bp (35), a similar degree of variation as that between two human
320 genomes. In our previous study we simply examined one time point (90 minutes
321 after drug treatment) and only looked at a single larval stage, the L1 stage — we
322 wanted to expand this analysis to compare the effects of KCN on N2 and CB4856
323 across development. We decided to examine how a range of concentrations of KCN
324 affect movement of all 4 larval stages of either N2 or CB4856 and in each case to
325 examine how this response evolves over 3hr (Fig 8).

326 The results are complex and striking. In keeping with our previous study (34), we
327 find that N2 are more affected by KCN at the L1 stage. However, we find the exact
328 reverse at the L4 stage — CB4856 are substantially more sensitive here. At the L3
329 stage, the picture is even more complex — while KCN appears to affect CB4856
330 more rapidly (CB4856 L3 animals are more severely affected at early timepoints),
331 the same dose of KCN has a more severe effect on N2 later timepoints. Taken
332 together, these data show clearly that comparisons of drug sensitivity in natural

333 populations are complex. It is impossible to make a blanket statement that isolate A
334 is 'more sensitive' than isolate B — assessing the effect at a different dose, a
335 different timepoint or a different developmental stage could give precisely the
336 reverse conclusion. These data underscore the need to measure drug responses as
337 comprehensively as possible before making general conclusions — without
338 measuring a range of doses and capturing these responses across time, we would
339 have missed much of this complexity.

340

341 Discussion

342 Drugs have extremely rapid effects on their targets — they can switch on or off their
343 target within minutes even in a whole animal. What is the effect on the animal and
344 how does it respond? We looked at the effects of drugs on *C.elegans* movement to
345 measure acute responses to drugs in a whole animal and find several unexpected
346 results that have important implications for drug screens in animals.

347 First, we found that around half of all the bioactive compounds that we found to
348 affect *C.elegans* movement show a complex response: the worms are rapidly
349 affected, but after an early phase of near-paralysis, the animals recover movement
350 — this recovery may be transient or longer lived. In some cases, like the responses
351 to compound shown in Fig 3E-F, we see multiple phases of paralysis and recovery
352 over time — studying these complex acute responses of worms over time will drive
353 exciting new insights. That worms can recover from the rapid effects of many drugs
354 indicates that the worms are responding in some way. We did not expect to see this

355 kind of recovery so frequently and to such a wide range of drugs and treatments, or
356 responses of such complexity — that surprise drove this study.

357 Second, at least in the examples we examined, the mechanisms underlying complex
358 acute responses appear to be drug specific and not due to a generic stress or
359 xenobiotic response. For example, recovery from paralysis due to signaling by one
360 set of acetylcholine receptors (AChRs) is due to signaling from a different set of
361 AChRs; recovery from paralysis due to inhibition of aerobic respiration is driven by
362 the use of anaerobic pathways. We see complex acute responses to a wide range of
363 drugs and thus worms can respond to many different acute perturbations of their
364 core networks by rewiring and modulating the activity of specific pathways. This
365 suggests a tremendous complexity of homeostatic mechanisms and sensors and this
366 molecular biology can be revealed through studying acute drug responses. For
367 example, worms recover from paralysis induced by activation of nAChRs through
368 signaling from mAChRs — this cross talk isn't evident in chronic drug assays but can
369 be easily measured using acute responses. Acute responses are thus excellent
370 reporters for the rewiring of genetic networks in response to the effects of a drug.

371 Finally, we find that many factors affect acute drug responses. The acute response to
372 the same drug can be very different at different developmental stages, at different
373 doses of drug, or in different individuals — measuring only a single dose, a single
374 time point, or a single developmental stage can greatly affect conclusions. For
375 example, we found that L1 larvae recover readily from Aldicarb-induced paralysis
376 but adults cannot recover. The recovery of L1s from Ald-induced paralysis is highly
377 dose-dependent — L1s do not recover at 2mM Ald but recover readily at the higher

378 concentration of 6mM (Fig 4A). This kind of complexity means one cannot simply
379 say '*C.elegans* can recover from Ald paralysis' or '*C.elegans* cannot recover from Ald
380 paralysis'. We see a similar complexity when we look at natural variation in acute
381 responses. We compared the sensitivity to KCN of two natural isolates of *C.elegans,*
382 N2 and CB4856 and find a complex picture — while N2 is more sensitive at the L1
383 stage, CB4856 is more sensitive at the L4 stage. Again, we cannot make a blanket
384 statement of 'N2 is more sensitive than CB4856' — dose, time point, and
385 developmental stage drive major differences in the drug responses and these factors
386 are often neglected. For example a GWAS to identify QTLs that affect 'drug
387 sensitivity' would likely find different variants depending on drug dose and
388 developmental stage assayed. Crucially, this means that to really understand acute
389 responses, we need to measure them over a range of doses and for each
390 developmental stage. The simple assay we report here allows us to gather this kind
391 of rich data.

392 Taken together, our results show that worms have complex acute responses to a
393 wide variety of drugs and that these complex responses are due to the specific
394 rewiring of the pathways underlying worm biology. Acute responses are sensitive
395 readouts of the pathways that are required after rewiring — some of these are
396 largely unexplored. For example, activation of mAChR signaling alone only has very
397 subtle effects on worm biology (36–40) but acute responses reveal a clear effect of
398 mAChR signaling in driving recovery from nAChR-induced paralysis. Genetic screens
399 to find mutants with altered acute drug responses can thus dissect otherwise
400 intractable pathways and acute responses can also be the basis for sensitive drug

401 screens. Understanding the genetics that underpin complex acute responses like
402 those shown in Fig 3 will reveal novel insights into how genetic networks rewire
403 and change following insult.

404 Importantly, we also show that acute drug responses vary in many ways — different
405 drug doses, different developmental stages, and different genetic backgrounds can
406 give very different acute responses. Drawing broad conclusions about drug
407 responses such as '*C.elegans* recovers from Aldicarb-induced paralysis' or 'the N2
408 isolate is more sensitive to KCN than the CB4856' is thus very difficult — different
409 doses or different developmental stages often give completely different results.
410 Studies on drugs in whole animals need to be aware of this complexity and interpret
411 results with care. We believe that high throughput quantitative assays for drug
412 responses of the kind we describe here are key — they allow researchers to build up
413 a rich view of a drug response rather than focus on an arbitrary dose, time point or
414 developmental stage. Studying the full complexity of acute responses opens up a
415 whole new set of whole animal phenotypes for drug and genetic screens and will
416 reveal how animals rapidly rewire their genetic networks in response to drugs,
417 toxins, and environmental stresses.

418 Materials and Methods

419 Worm Maintenance and Strains

420 All worm stocks were maintained at 20ºC on NGM agar plates seeded with *E.coli*
421 strain OP50 as described elsewhere (41). In addition to the classical laboratory
422 strain N2, we describe work using strains *unc-38* (*e264)*, *lev-8* (*x15*), *lev-1* (*e211*),

423 *unc-63* (*x26*), *unc-29* (*e1072*), *acr-8* (*ok1240*), *acr-16* (*ok789*), *gar-1* (*ok755*), *gar-2*
424 (*ok520*) and *gar-3* (*gk305*). All strains were acquired from the Caenorhabditis
425 Genetics Center.
426 To prepare L1 worms, animals were washed from the agar plates with M9 buffer
427 (41) and rinsed in one buffer change of M9. L1s were then isolated by filtration
428 though 11 µm nylon mesh filter plates (Milipore Multiscreen). L1 larvae for
429 immediate use in drug response assays were diluted to approximately 1.2 worms
430 per microlitre in either M9 buffer or modified NGM buffer (50 mM NaCl, 1 mM $CaCl_2$,
431 1mM $MgSO_4$, 200 mM KH2PO4, 50 mM K_2HPO_4).
432 To assay drug response over different developmental stages, worm populations
433 were first developmentally synchronized by filtration of L1s, as described above.
434 Filtered L1s were returned to fresh NGM agar OP50 plates and incubated at 20ºC
435 until they had reached the required developmental stage (L1: no further incubation,
436 L2: 18 hr, L3: 32 hr, L4: 42 hr, young adult: 54 hrs). Worms were then washed from
437 the plates and rinsed as above. To further synchronize developmental stages, worms
438 were dispensed into assay wells using a COPAS Biosort machine (Union Biometrica),
439 which can selectively dispense individual worms on the developmentally-correlated
440 criteria of size and optical density (L1 worms: 100 / well, L2: 80 / well, L3:, 50 /
441 well, L4: 30 / well, young adult : 30 / well). Sorting parameters for each stage were
442 determined empirically, as per the manufacturer's instructions. The volume of liquid
443 dispensed into the wells was determined and adjusted to 100 µl with buffer.
444

445 ## Drug preparation

446 Solutions of potassium cyanide (Sigma Aldrich 60178-25G), sodium chloride
447 (BioShop SOD002.205), cycloheximide (Sigma Aldrich C7698-1G) abamectin (Sigma
448 Aldrich 31732) and 2-dexoxy-D-glucose (Sigma Aldrich D8375) were prepared fresh
449 to twice the working concentration in M9 buffer, 1.6% DMSO. Stock solutions of
450 aldicarb (Sigma Aldrich, 33386) were prepared to 1 M in DMSO. Solutions of
451 levamisole hydrochloride (Acros Organics, 16595-80-5), oxotremorine M (Sigma
452 Aldrich, O100) and mecamylamine hydrochloride (Sigma Aldrich, M9020) were
453 prepared to 100 mM in water. These solutions were divided into single use aliquots
454 and frozen. Stocks of arecoline hydrobromide (Acros Organics, 250130050) and
455 atropine sulphate monohydrate (Sigma Aldrich, A0257) were prepared fresh on the
456 day of use in M9 buffer. (-)-Nicotine (Sigma Aldrich, N3876) was stored frozen,
457 undiluted in single use aliquots.

458 ## Preparation of drug response assays:

459 Assays were assembled in a final volume of 200 µl in flat-bottomed, polystyrene 96-
460 well plates (Corning 3997) by combining 100 µl of worms in buffer with an equal
461 volume of drug solution. To control for any confounding effects of drug solvent, all
462 experiments were prepared to contain DMSO at 0.8 % v/v, regardless of whether
463 the drug solution was prepared in DMSO or water. All assays were assembled in M9
464 buffer apart from the screen for compounds that modify the response to aldicarb,
465 which were assembled in modified NGM, which we found to cause fewer problems
466 of drug precipitation. After assembling the assay, plates were sealed with

467 transparent, self-adhesive films before imaging. The point at which worms and
468 drugs were combined marked the start of the assay.

469 ### Preparation of RNAi assays

470 RNAi-by-feeding was performed as previously described (42). After 4 days, RNAi-
471 treated and mock-treated worms were filtered to purify L1 worms and washed in
472 two buffer changes of M9. Purified L1 samples were diluted to approximately 1.2
473 worms per microlitre and 100 µl samples were transferred to microtitre plates for
474 use in mobility assays.

475 ### Image acquisition, analysis and calculation of fractional mobility score:

476 Images were acquired using a Nikon Ti Eclipse inverted microscope with 2x
477 objective lens and DS-Qi1Mc camera. Image capture was automated in Nikon NIS-
478 Elements AR software to capture two images of each well, separated by a 500 ms
479 interval. This procedure was run in a 5 minute loop for the 3 hour duration of the
480 experiments. A sample NIS-elements script is available as supplementary
481 information.

482 Since our microscope control software stores files in a proprietary image stack
483 format (Nikon ND2), we began our image analysis with a file format conversion
484 process to convert nd2 files to a collection of 8-bit TIFF images, with structured
485 filenames identifying the timepoint and well coordinates of each image. The first
486 step of this process, defined in the Python file *export_nd2.py*, converted the ND2 file
487 to a series of TIFF files, using the Open Microscopy Environment Bio-Formats tool
488 (43). This conversion yields a series of 12-bit TIFF files with names encoding the
489 timepoint and order of acquisition of each image. The second step of the conversion

490 process invoked the ImageMagick package to convert these files from 12-bit to 8-bit
491 TIFF, modify filenames to include the well location, rather than order of acquisition
492 and group files for each timepoint into separate subfolders. This file structure forms
493 the input for the image analysis script.
494 Our image analysis pipeline was prepared with the python programming language
495 using the scikit-image library (44). All images were first processed with a Gaussian
496 blur to reduce noise levels. Further image analysis consisted of two sets of processes
497 to find moving and non-background, non-moving parts of the images.
498 To identify non-background, non-moving pixels, images were processed using a
499 Sobel filter, which effectively produces the first derivative of the image, thus edges
500 are highlighted and sharper edges appear brighter than shallow edges. An adaptive
501 threshold was applied to the Sobel images to remove the background and yield a
502 binary image. These binary images contained the outlines of the well and any
503 objects, such as worms, within the well. Binary images were further processed with
504 two iterations of binary closing to fill the pixels between sufficiently close edges.
505 This process was hand-tuned to fill in the area occupied by worms but minimize
506 overfilling into the areas between worms. A circular binary mask was applied to
507 remove the edges of the wells from each binary image and one of these images was
508 designated as a reference image for each well (Figure 1A, Image B).
509 Pixels associated with movement were identified by calculating the absolute
510 difference of the two consecutive images of a well (Figure 1A, Image A). A threshold
511 was applied to the difference image to create a binary image (Figure 1A, Image B).
512 This binary image contained the moving pixels from both parent images, showing

513 double the number of movement-associated pixels. To correct for this, we multiplied
514 the binary difference image by the reference image described above revealing only
515 the non-background, movement associated pixels from a single frame (Figure 1A,
516 Image C). Finally to identify pixels that did not move between wells, the reference
517 image was multiplied by the complement of Image C (Figure 1A, Image D).
518 A fractional mobility score was calculated as the ratio of movement-associated
519 pixels to total non-background pixels. This process is contained in the Python script
520 *quantify_movement.py*. A second Python script, *quantify_movement_adult.py*, was
521 used to analyse images of adult worms. This script contains an additional step to
522 mask out objects below a certain number of pixels in size, to remove eggs from the
523 analysis, since some chemicals stimulate egg-laying.
524 All our python scripts and an example dataset are available in our repository,
525 https://github.com/fraser-lab-UofT/acute_assay

526 ### Data analysis and curve-fitting:

527 All drug response data shown were normalised by dividing by the fractional
528 mobility score of drug-free control wells for each time point. Fitted lines were
529 determined by least squares minimisation of either a three-parameter logistic
530 function:

531 $$f(x) = A + \frac{1 - A}{1 + e^{-B(M-x)}}$$

532 or an exponential function:

533 $$f(x) = Me^{-x} + A$$

534 Where x denotes drug concentration and M, A and B denote parameters to be

535 optimized. The choice of function was determined by the range of the dataset.

536

537 Proportional recovery scores were calculated using the formula:

538 $$\frac{(FMS\ after\ recovery - FMS\ at\ maximum\ paralysis)}{1 - FMS\ at\ maximum\ paralysis}$$

539 The value of FMS after recovery was calculated as the mean FMS over the period

540 between 150 and 180 minutes. Maximum paralysis was determined as the minimum

541 FMS value over the three hour course of the experiment.

542 References

543 1. Lewis JA, Wu CH, Berg H, Levine JH. The genetics of levamisole resistance in

544 the nematode Caenorhabditis elegans. Genetics. 1980 Aug;95(4):905–28.

545 2. Driscoll M, Dean E, Reilly E, Bergholz E, Chalfie M. Genetic and molecular

546 analysis of a Caenorhabditis elegans beta-tubulin that conveys benzimidazole

547 sensitivity. J Cell Biol. 1989 Dec;109(6 Pt 1):2993–3003.

548 3. Dent JA, Smith MM, Vassilatis DK, Avery L. The genetics of ivermectin

549 resistance in Caenorhabditis elegans. Proc Natl Acad Sci U S A. 2000 Mar

550 14;97(6):2674–9.

551 4. Jones AK, Buckingham SD, Sattelle DB. Chemistry-to-gene screens in

552 Caenorhabditis elegans. Nat Rev Drug Discov. 2005 Apr;4(4):321–30.

553 5. Brenner S. The genetics of Caenorhabditis elegans. Genetics. 1974

554 May;77(1):71–94.

555 6. Nguyen M, Alfonso A, Johnson CD, Rand JB. Caenorhabditis elegans mutants

556 resistant to inhibitors of acetylcholinesterase. Genetics. 1995;140(2):527–35.
557 7. Miller KG, Alfonso A, Nguyen M, Crowell JA, Johnson CD, Rand JB. A genetic
558 selection for Caenorhabditis elegans synaptic transmission mutants. Proc Natl
559 Acad Sci U S A. 1996 Oct 29;93(22):12593–8.
560 8. Rogalski TM, Golomb M, Riddle DL. Mutant Caenorhabditis elegans RNA
561 polymerase II with a 20,000-fold reduced sensitivity to alpha-amanitin.
562 Genetics. 1990 Dec;126(4):889–98.
563 9. Kwok TCY, Ricker N, Fraser R, Chan AW, Burns A, Stanley EF, et al. A small-
564 molecule screen in C. elegans yields a new calcium channel antagonist. Nature.
565 2006 May 4;441(7089):91–5.
566 10. Burns AR, Kwok TCY, Howard A, Houston E, Johanson K, Chan A, et al. High-
567 throughput screening of small molecules for bioactivity and target
568 identification in Caenorhabditis elegans. Nat Protoc. 2006 Nov;1(4):1906–14.
569 11. Kwok TCY, Hui K, Kostelecki W, Ricker N, Selman G, Feng Z-P, et al. A Genetic
570 Screen for Dihydropyridine (DHP)-Resistant Worms Reveals New Residues
571 Required for DHP-Blockage of Mammalian Calcium Channels. Frankel WN,
572 editor. PLoS Genet. 2008 May 9;4(5):e1000067.
573 12. Luciani GM, Magomedova L, Puckrin R, Urbanus ML, Wallace IM, Giaever G, et
574 al. Dafadine inhibits DAF-9 to promote dauer formation and longevity of
575 Caenorhabditis elegans. Nat Chem Biol. 2011 Dec 6;7(12):891–3.
576 13. Burns AR, Luciani GM, Musso G, Bagg R, Yeo M, Zhang Y, et al. Caenorhabditis
577 elegans is a useful model for anthelmintic discovery. Nat Commun. 2015 Jun
578 25;6:7485.

579 14. Buckingham SD, Sattelle DB. Fast, automated measurement of nematode
580 swimming (thrashing) without morphometry. BMC Neurosci. 2009 Jul
581 20;10(1):84.
582 15. Brown AEX, Yemini EI, Grundy LJ, Jucikas T, Schafer WR. A dictionary of
583 behavioral motifs reveals clusters of genes affecting Caenorhabditis elegans
584 locomotion. Proc Natl Acad Sci. 2013 Jan 8;110(2):791–6.
585 16. Yemini E, Kerr RA, Schafer WR. Tracking Movement Behavior of Multiple
586 Worms on Food. Cold Spring Harb Protoc. 2011 Dec
587 1;2011(12):pdb.prot067025.
588 17. Yemini E, Jucikas T, Grundy LJ, Brown AEX, Schafer WR. A database of
589 Caenorhabditis elegans behavioral phenotypes. Nat Methods. 2013 Sep
590 14;10(9):877–9.
591 18. Larsch J, Ventimiglia D, Bargmann CI, Albrecht DR. High-throughput imaging
592 of neuronal activity in Caenorhabditis elegans. Proc Natl Acad Sci. 2013 Nov
593 5;110(45):E4266–73.
594 19. Swierczek NA, Giles AC, Rankin CH, Kerr RA. High-throughput behavioral
595 analysis in C. elegans. Nat Methods. 2011;8(7):592-U112.
596 20. Rand J. Acetylcholine. The C. elegans Research Community, editor.
597 WormBook. 2007. 1-21 p.
598 21. Richmond JE, Jorgensen EM. One GABA and two acetylcholine receptors
599 function at the. Nat Neurosci. 1999;2(9):791–8.
600 22. Opperman CH, Chang S. Effects of Aldicarb and Fenamiphos on
601 Acetycholinesterase and Motility of Caenorhabditis elegans. J Nematol. 1991

602 Jan;23(1):20–7.
603 23. Fleming JT, Squire MD, Barnes TM, Tornoe C, Matsuda K, Ahnn J, et al.
604 Caenorhabditis elegans levamisole resistance genes lev-1, unc-29, and unc-38
605 encode functional nicotinic acetylcholine receptor subunits. J Neurosci. 1997
606 Aug 1;17(15):5843–57.
607 24. Culetto E, Baylis HA, Richmond JE, Jones AK, Fleming JT, Squire MD, et al. The
608 Caenorhabditis elegans unc-63 gene encodes a levamisole-sensitive nicotinic
609 acetylcholine receptor alpha subunit. J Biol Chem. 2004 Oct 8;279(41):42476–
610 83.
611 25. Towers PR, Edwards B, Richmond JE, Sattelle DB. The Caenorhabditis elegans
612 lev-8 gene encodes a novel type of nicotinic acetylcholine receptor alpha
613 subunit. J Neurochem. 2005 Apr;93(1):1–9.
614 26. Boulin T, Gielen M, Richmond JE, Williams DC, Paoletti P, Bessereau J-L. Eight
615 genes are required for functional reconstitution of the Caenorhabditis elegans
616 levamisole-sensitive acetylcholine receptor. Proc Natl Acad Sci.
617 2008;105(47):18590–5.
618 27. Lee YS, Park YS, Chang DJ, Hwang JM, Min CK, Kaang BK, et al. Cloning and
619 expression of a G protein-linked acetylcholine receptor from Caenorhabditis
620 elegans. J Neurochem. 1999 Jan;72(1):58–65.
621 28. Hwang JM, Chang DJ, Kim US, Lee YS, Park YS, Kaang BK, et al. Cloning and
622 functional characterization of a Caenorhabditis elegans muscarinic
623 acetylcholine receptor. Receptors Channels. 1999;6(6):415–24.
624 29. Lee YS, Park YS, Nam S, Suh SJ, Lee J, Kaang BK, et al. Characterization of GAR-

625 2, a novel G protein-linked acetylcholine receptor from Caenorhabditis
626 elegans. J Neurochem. 2000 Nov;75(5):1800–9.
627 30. Ishii M, Kurachi Y. Muscarinic acetylcholine receptors. Curr Pharm Des.
628 2006;12(28):3573–81.
629 31. Hanstein WG. Uncoupling of oxidative phosphorylation. Biochim Biophys
630 Acta. 1976 Sep 27;456(2):129–48.
631 32. Ghosh R, Andersen EC, Shapiro J a, Gerke JP, Kruglyak L. Natural Variation in a
632 Chloride. Science (80-). 2012;335(February):574–8.
633 33. Zdraljevic S, Strand C, Seidel HS, Cook DE, Doench JG, Andersen EC. Natural
634 variation in a single amino acid substitution underlies physiological responses
635 to topoisomerase II poisons. Macdonald SJ, editor. PLoS Genet. 2017 Jul
636 12;13(7):e1006891.
637 34. Vu V, Verster AJAJ, Schertzberg M, Chuluunbaatar T, Spensley M, Pajkic D, et
638 al. Natural Variation in Gene Expression Modulates the Severity of Mutant
639 Phenotypes. Cell. 2015;162(2):391–402.
640 35. Wicks SR, Yeh RT, Gish WR, Waterston RH, Plasterk RH. Rapid gene mapping
641 in Caenorhabditis elegans using a high density polymorphism map. Nat Genet.
642 2001 Jun 1;28(2):160–4.
643 36. Steger KA, Avery L. The GAR-3 muscarinic receptor cooperates with calcium
644 signals to regulate muscle contraction in the Caenorhabditis elegans pharynx.
645 Genetics. 2004 Jun 1;167(2):633–43.
646 37. Liu Y, LeBoeuf B, Garcia LR. G alpha(q)-coupled muscarinic acetylcholine
647 receptors enhance nicotinic acetylcholine receptor signaling in

648 Caenorhabditis elegans mating behavior. J Neurosci. 2007 Feb 7;27(6):1411–
649 21.
650 38. Dittman JS, Kaplan JM. Behavioral impact of neurotransmitter-activated G-
651 protein-coupled receptors: muscarinic and GABAB receptors regulate
652 Caenorhabditis elegans locomotion. J Neurosci. 2008;28(28):7104–12.
653 39. Chan JP, Staab TA, Wang H, Mazzasette C, Butte Z, Sieburth D. Extrasynaptic
654 muscarinic acetylcholine receptors on neuronal cell bodies regulate
655 presynaptic function in Caenorhabditis elegans. J Neurosci. 2013 Aug
656 28;33(35):14146–59.
657 40. Hendricks M, Ha H, Maffey N, Zhang Y. Compartmentalized calcium dynamics
658 in a C. elegans interneuron encode head movement. Nature.
659 2012;487(7405):99–103.
660 41. Stiernagle T. Maintenance of C. elegans. In: The C. elegans Research
661 Community, editor. Wormbook. 2006.
662 42. Lehner B, Crombie C, Tischler J, Fortunato A, Fraser AG. Systematic mapping
663 of genetic interactions in Caenorhabditis elegans identifies common modifiers
664 of diverse signaling pathways. Nat Genet. 2006;38(8):896–903.
665 43. Moore J, Linkert, Melissa Blackburn, Colin Carroll, Mark Ferguson RK, Flynn H,
666 Gillen K, Leigh R, Li S, et al. OMERO and Bio-Formats 5: flexible access to large
667 bioimaging datasets at scale. Proc SPIE 9413, Med Imaging 2015 Image
668 Process. 2015;941307.
669 44. van der Walt S, Schönberger J, Nunez-Iglesias, J Boulogne F, Warner J, Yager N,
670 Gouillart E, et al. scikit-image: Image Processing in Python. PeerJ.

2014;(2):e423.

674 ## Figure Captions

675

676 **Figure 1: Outline of an image-based assay for worm mobility**

677 **A:** Worms are placed in a 96 well plate in M9 buffer and treated with drugs as
678 required. Two images of each well (Im1 and Im2) are captured at an interval of 500
679 ms at each timepoint. Images are processed as described in Materials and Methods
680 to identify portions of the worms that move between the two images (green) and
681 parts that remain stationary (red). This allows the calculation of a raw fractional
682 mobility score (F.M.S.) as the fraction of total worm-associated pixels (red and
683 green) that moved (green). This processing is illustrated in a magnified region of
684 Im1 and Im2 (defined by blue box). **B: The image-based assay produces a rich**
685 **view of drug effects on worm movement.** L4 worms were treated with a range of
686 doses of aldicarb and movement measured at 5 minute time points over a 3 hour
687 time course. The heat map shows the F.M.S. for each drug dose at each timepoint —
688 white indicates full movement, red indicates lack of movement. Either dose
689 response curves at a given time point (pink arrow) or kinetic responses to a single
690 drug dose (red and blue arrows) can be extracted from these rich data. Data are
691 means of four independent experiments. Error bars show standard error of the
692 mean.

693

694 **Figure 2: Assay characterisation.**

695 **A: Effect of aldicarb on adult worms:** Adult worms were treated with aldicarb at a
696 range of concentrations and FMS was calculated at 5 minute intervals. FMS was

697 plotted as a time-course of response for each concentration. **B: Adult worms**
698 **homozygous for a loss-of-function *unc-38*(*e264*) mutation are insensitive to**
699 **aldicarb.** A-C show means of 4 independent experiments; error bars show standard
700 error of the mean. All data are normalised to drug-free controls.**C: The dose-**
701 **response relationship for aldicarb is affected by addition of mecamylamine,**
702 **an antagonist of nAChRs.** EC50 values were calculated by fitting a 3-parameter
703 logistic function to the data (see Materials and Methods). **D: Assay detects effects**
704 **of targeting genes required for normal movement using RNAi.** L1 worms were
705 grown for 4 days in the presence of *E. coli* strains expressing dsRNA that target
706 individual genes known to be required for normal movement. L1 progeny from
707 these cultures were isolated by filtration and their mobility quantified using our
708 assay. Mobility scores are normalized to a non-targeting RNAi control (dsRNA
709 targeted against GFP). Data represent the mean of 8 wells, containing 100 worms
710 per well.
711
712 **Figure 3: A wide range of compounds elicit movement responses.**
713 L1 worms were exposed to a range of doses of various compounds and movement
714 quantified. **A: Effect of potassium cyanide on L1 worms.** Data are means of 4
715 independent replicates. **B: Effect of cycloheximide on L1 worms.** Data are means
716 of 3 independent replicates. **C: Effect of sodium chloride on L1 worms**. Data are
717 means of 4 independent replicates. **D: Effect of abamectin on L1 worms.** Data are
718 means of 4 independent replicates. **E-G: Novel compounds elicit a range of**
719 **dynamic responses.** Time-resolved responses for a number of novel compounds

720 elicited a range of different response dynamics. L1 worms were continuously
721 exposed to 40 μM of each compound. Data are means of 3 independent replicates.
722 (**A-G)** Error bars show standard error of the mean.
723
724 **Figure 4: Larval worms show dose-dependent recovery from cholinergic**
725 **paralysis.**
726 **A: Timecourse of response to 4mM aldicarb at different developmental stages**.
727 Worms from each developmental stage were purified and dispensed using a COPAS
728 biosort worm sorter before exposure to aldicarb as in Figure 2. Early larval stages
729 show a robust recovery from paralysis, whereas L4 and adult worms show little
730 recovery. Data are means of 3 independent experiments. **B: Response of L1 worms**
731 **to nicotine.** L1 worms were treated with a range of nicotine concentrations and
732 FMS measured over a 3hr time course. Data are means of 4 independent
733 experiments. **C: Recovery of L1 worms from Ald-induced paralysis increases**
734 **with higher doses**. For each concentration shown, a proportional recovery value
735 was calculated as described in Material and Methods. Data are means of four
736 independent experiments. **D: Recovery of L1 worms from Nic-induced paralysis**
737 **decrease with higher doses**. Proportional recovery scores were calculated as
738 above. Data are means of three independent experiments. **A-D:** Error bars show
739 standard error of the mean.
740
741 **Figure 5: L1 cholinergic recovery can be modified by compounds with**
742 **muscarinic activity.**

743 **A: The recovery from Ald-paralysis is suppressed by the mAChR antagonist**
744 **Atr**. L1 worms were treated with 4mM Ald along with a range of doses of Atropine
745 (Atr); FMS was measured every 5mins over a 3hr time course.
746 **B: *gar-3* mutants show greatly reduced recovery from Ald-induced paralysis**.
747 Wild-type animals, or worms homozygous for mutations in either *gar-1, gar-2,* or
748 *gar*-3 were exposed to 4mM Ald and FMS measured across a 3hr time course.
749 **C: Aldicarb induces recovery from nicotine-induced paralysis in L1 larvae**.
750 Various concentrations of aldicarb were combined with a concentration of nicotine
751 sufficient to cause sustained paralysis (10 mM, shown in blue). Increasing
752 concentrations of aldicarb stimulated increasing degrees of recovery from paralysis.
753 **D: The mAChR-specific agonist OxoM similarly stimulates recovery from Nic-**
754 **induced paralysis**. L1 animals were treated with 10mM Nic combined with a range
755 of concentrations of OxoM. **E: OxoM-induced recovery requires *gar-3*:** Wild-type
756 animals, or worms homozygous for mutations in either *gar-1, gar-2,* or *gar*-3 were
757 exposed to 10mM Nic and 10mM OxoM and FMS measured across a 3hr time course.
758 The shaded portion represents the range of responses of N2, *gar-1, gar-2* and *gar-3*
759 to nicotine, in the absence of OxoM. **(A-E)** All data are means of 4 independent
760 experiments, normalized to no drug controls. Error bars show standard error of the
761 mean. **F: OxoM-does not induce recovery from Ald paralysis in adult worms:**
762 **requires *gar-3*:** Adult worms were exposed to 5mM Ald, with or without 10mM
763 OxoM. The presence of OxoM does not induce recovery from Ald-mediated paralysis
764 in adult worms. Data are means of three independent experiments; error bars show
765 standard error of the mean.

766

767 **Figure 6: Conceptual model of cholinergic responses in L1 *C. elegans***

768 **A:** Nic alone causes paralysis through binding to nAChRs. **B:** The paralysis caused by
769 the action of Nic at nAChRs in relieved by the action of OxoM at mAChRs. **C:** By
770 elevating levels of ACh, Ald treatment leads to transient paralysis by activation of
771 nAChRs, followed by recovery from paralysis, mediated by the action of ACh on
772 mAChRs.

773

774 **Figure 7 Dose sensitivity to KCN is complex.**

775 **A: L1 worms were treated with a range of KCN doses and their movement**
776 **measured over time.** The Fractional Mobility Scores (FMS) are shown at various
777 time points. At early time points the dose response curves are complex —
778 intermediate doses cause more severe movement defects than high doses. **B:**
779 **Decreased sensitivity to KCN at higher doses is dependent on a metabolic**
780 **transition to glycolysis.** Inhibition of glycolysis with 2-dexoy-D-glucose causes
781 higher-doses of KCN to be more toxic than lower doses, in contrast to the dose-
782 response relationship of KCN alone. This suggests that the relatively mild effects of
783 higher KCN concentrations seen in panel A is at least partially attributable to KCN
784 stimulating a shift in metabolic pathways from oxidative phosphorylation to
785 glycolysis. Data shown are at the 20 minute time point. **A-B:** Curves show mean of 3
786 repeats; error bars are standard error of the mean.

787

788 **Figure 8 Variation in dose sensitivity to KCN changes across development.**

789 **A:** Worms of specific stages of either N2 or CB4856 isolates were purified using a
790 worm sorter. Worms are sorted based on length and darkness — the exact windows
791 chosen are indicated by coloured boxes and examples of the sorted worms shown.
792 **B:** N2 or CB4856 worms of specific developmental stages were exposed to a range of
793 doses of KCN and their movement measured over a 3hr time course. The fractional
794 mobility score (F.M.S.) was calculated at each time point. The figure shows the
795 difference in F.M.S. scores for N2 and CB4856 — blue colours indicate that N2 has a
796 lower score, red colours that CB4856 is moving less.
797
798 **Figure S1: Response of nAChR subunit mutants to aldicarb in L1 worms**
799 Several nAChR subunits are required for wild-type sensitivity of L1 worms to 8mM
800 aldicarb, including UNC-29, UNC-63, LEV1, LEV-8 and UNC-38. ACR-16 and ACR-8
801 are not required for Ald-sensitivity in adults. All data are means of 3 independent
802 replicates. Error bars are standard error of the mean.
803 **Figure S2: Further characterisation of mAChR recovery**
804 Arecoline (Are), a mAChR agonist induces recovery from paralysis under 10 mM Nic
805 in the same manner as OxoM. Data are means of 4 wells. Error bars are standard
806 error of the mean.
807
808 **Figure S3: Time course of response of L1 worms to a range of Ald**
809 **concentrations.** Data are means of 4 independent experiments. Error bars are
810 standard error of the mean.

Figure 1

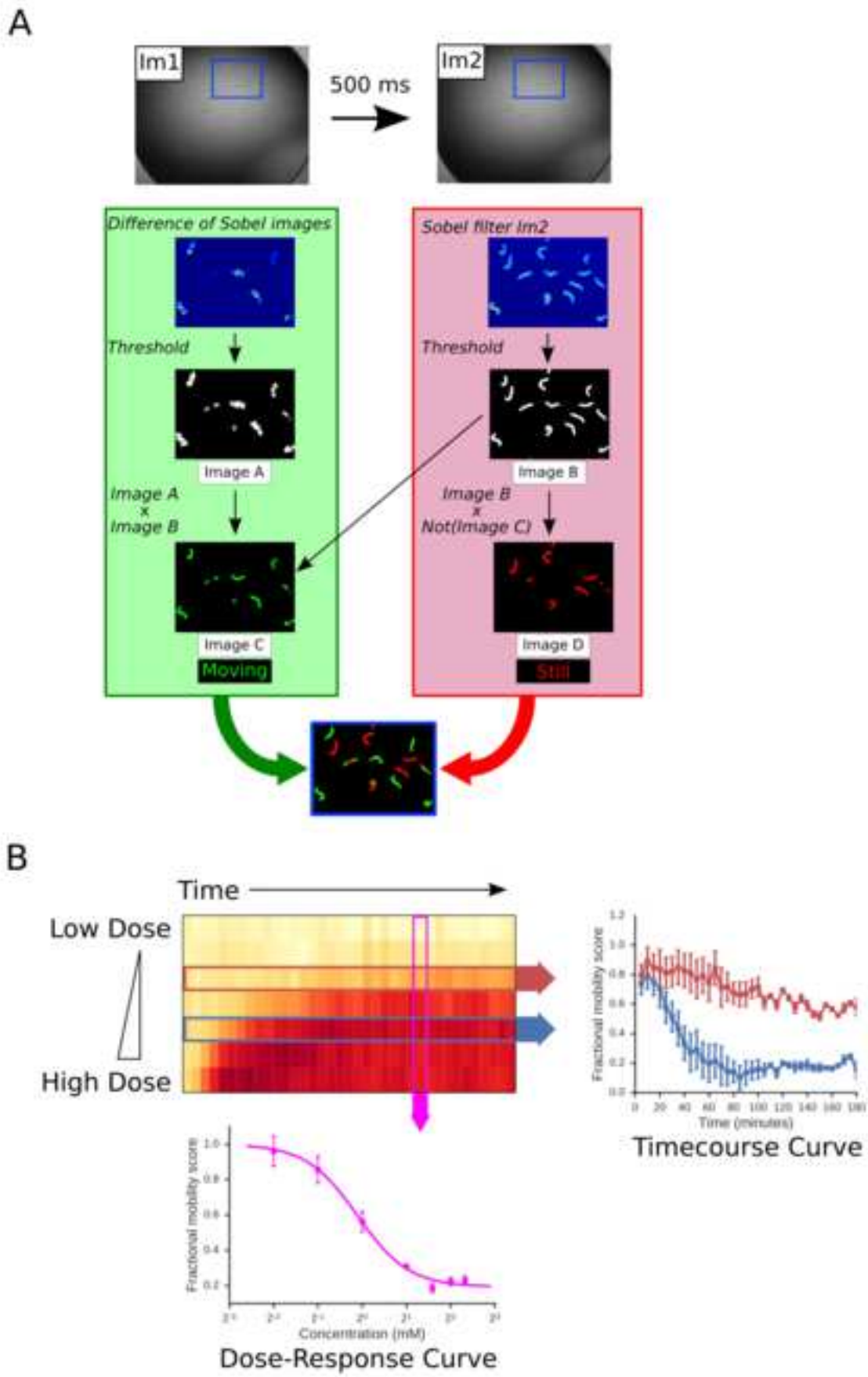
A
Im1
500 ms
Im2
Difference of Sobel images
Threshold
Image A
Image A
x
Image B
Image C
Moving
Sobel filter Im2
Threshold
Image B
Image B
x
Not(Image C)
Image D
Still
B
Time
Low Dose
High Dose
Fractional mobility score
Time (minutes)
Timecourse Curve
Fractional mobility score
Concentration (mM)
Dose-Response Curve

Click here to download Figure fig2.tif

Figure 2

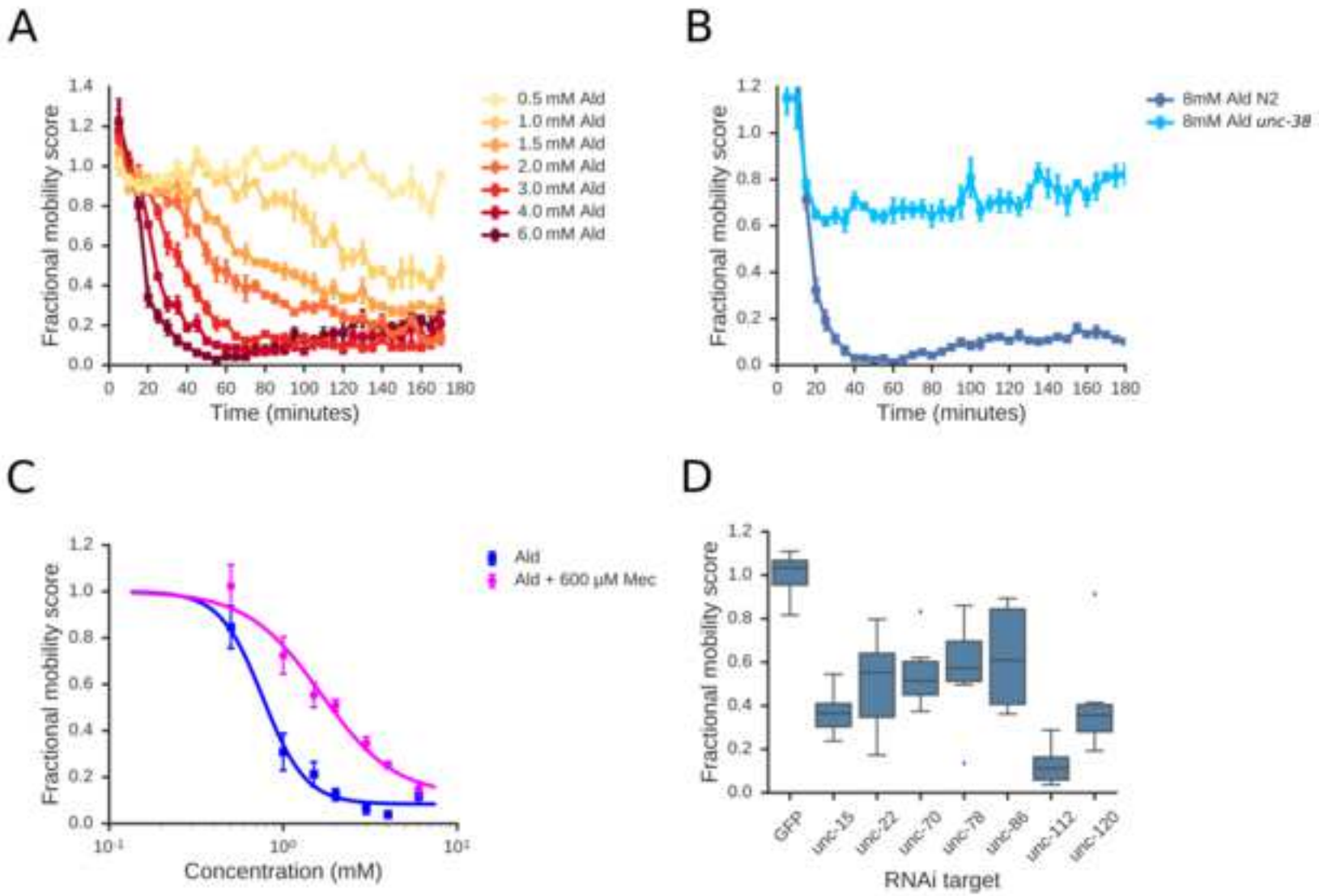

Click here to download Figure fig3.tif

Figure 3

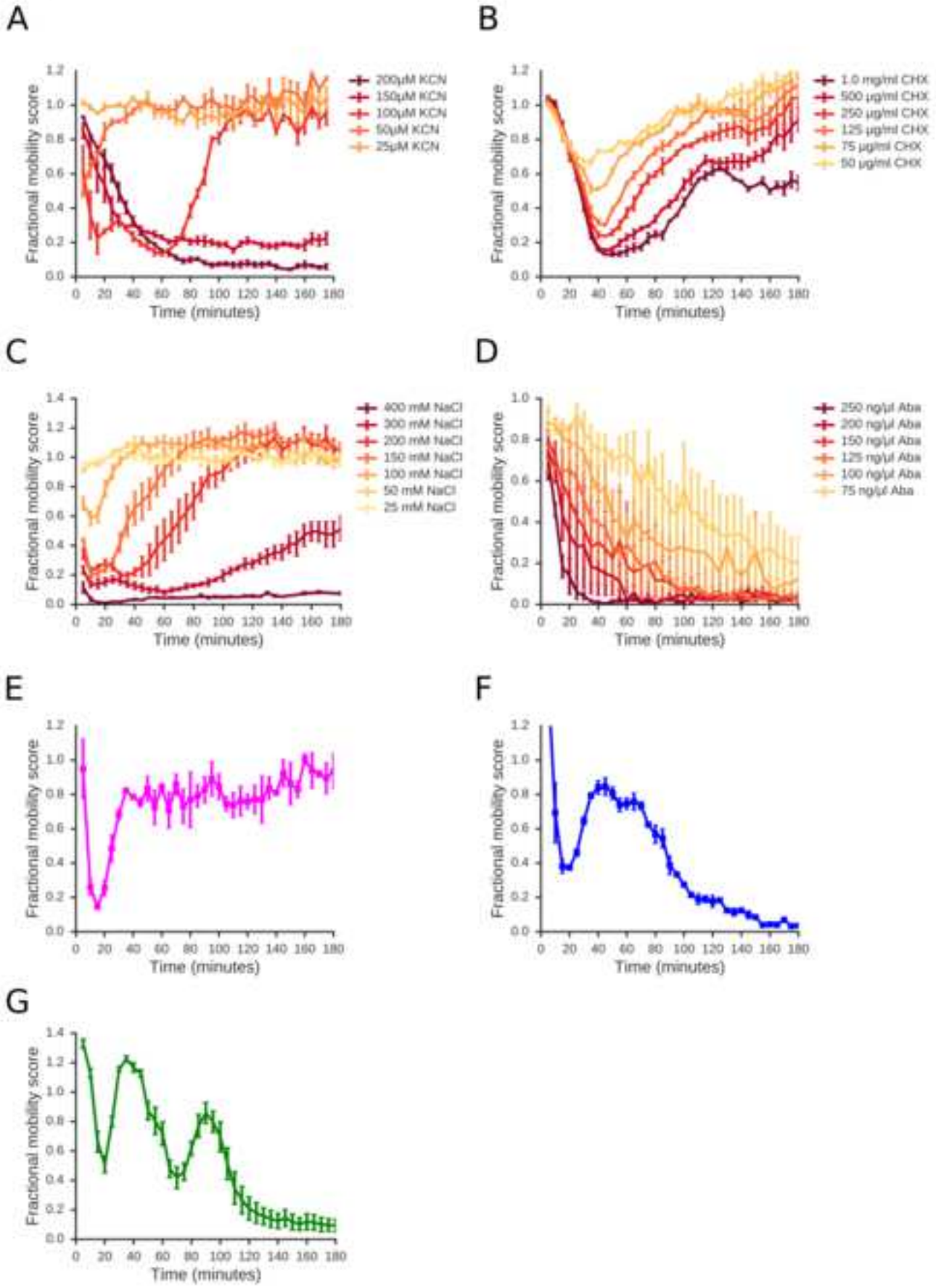

Click here to download Figure fig4.tif

Figure 4

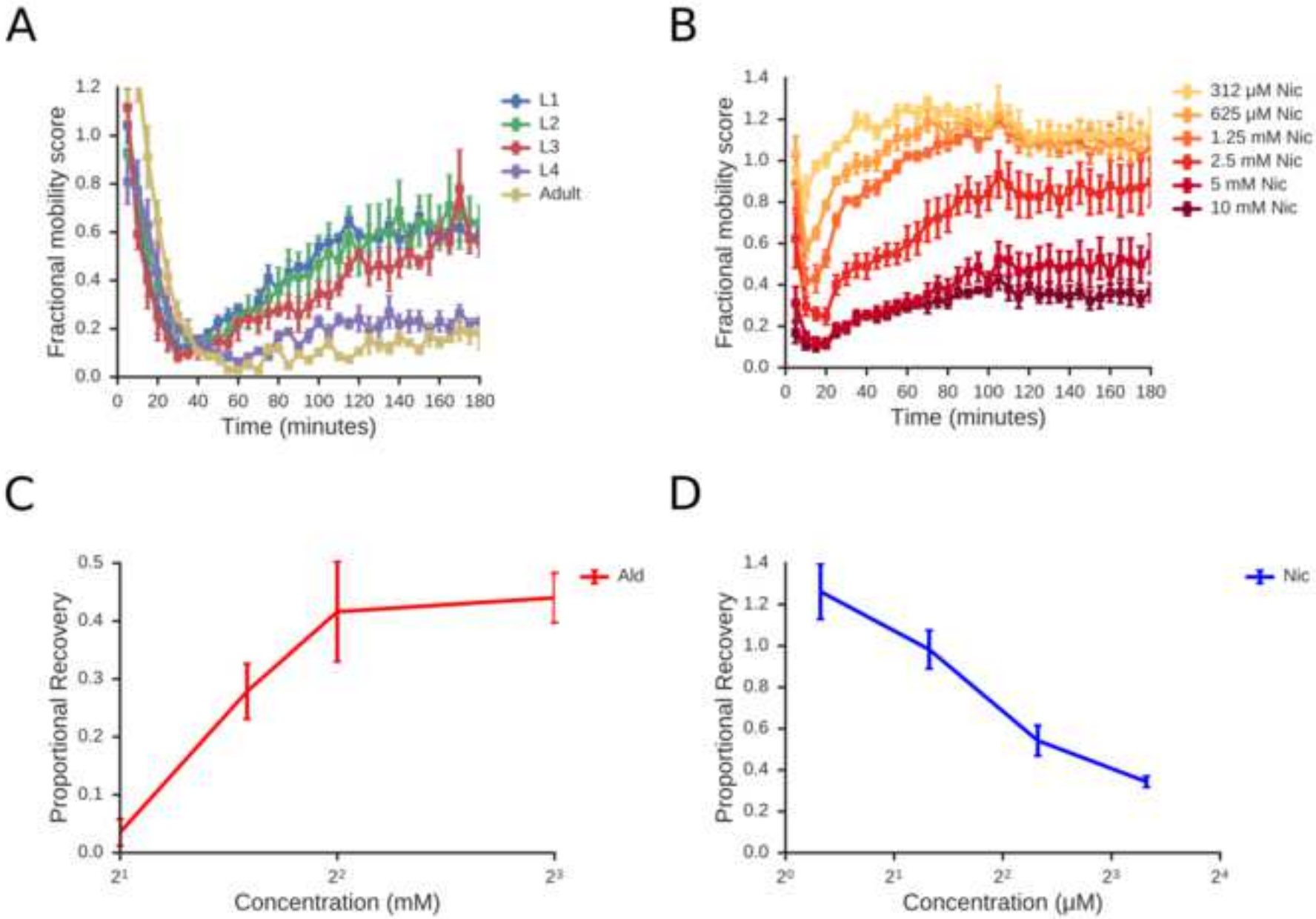

Figure 5

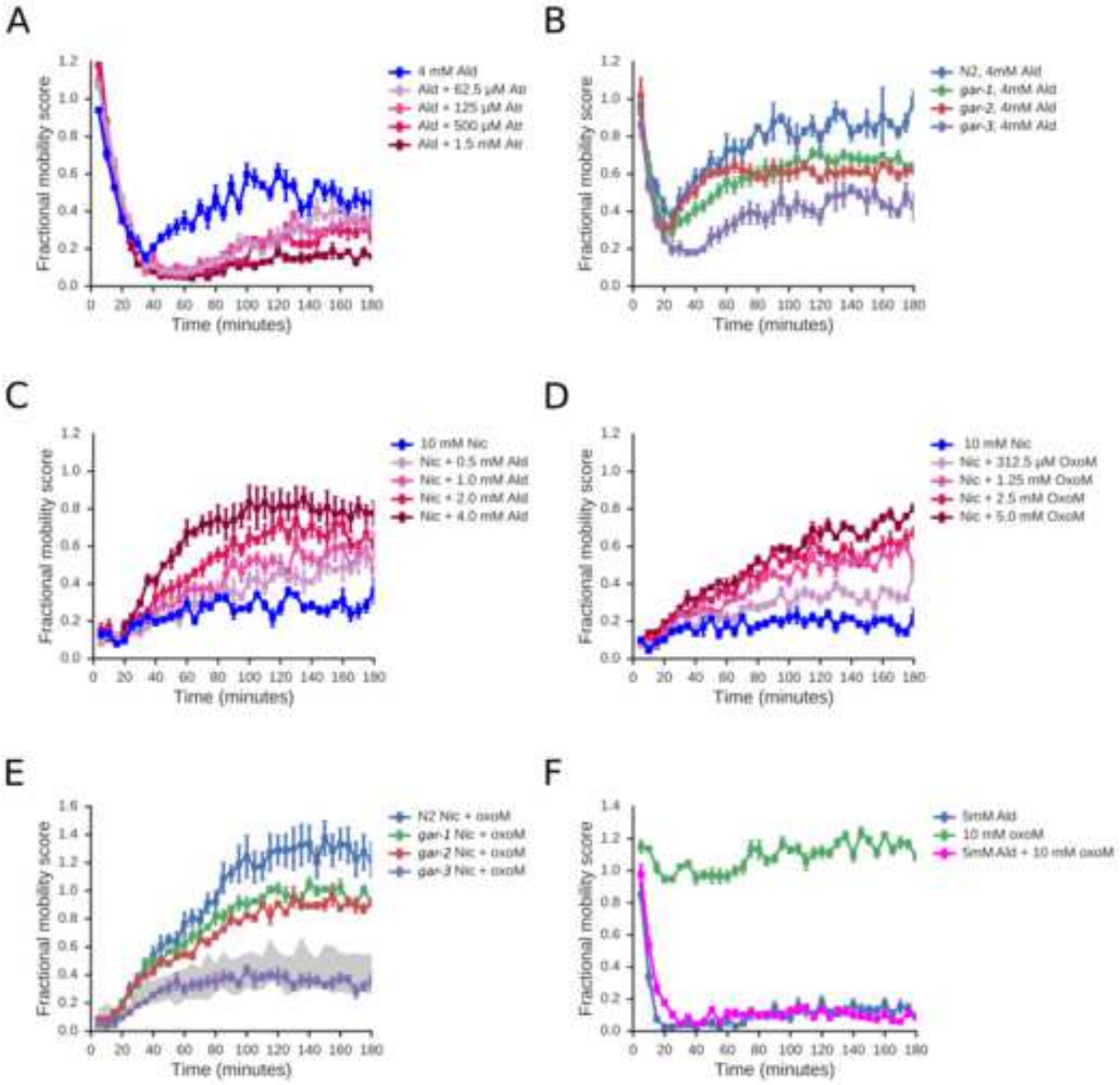
A
Fractional mobility score
Time (minutes)
4 mM Ald
Ald + 62.5 μM Atr
Ald + 125 μM Atr
Ald + 500 μM Atr
Ald + 1.5 mM Atr
B
Fractional mobility score
Time (minutes)
N2, 4mM Ald
gar-1, 4mM Ald
gar-2, 4mM Ald
gar-3, 4mM Ald
C
Fractional mobility score
Time (minutes)
10 mM Nic
Nic + 0.5 mM Ald
Nic + 1.0 mM Ald
Nic + 2.0 mM Ald
Nic + 4.0 mM Ald
D
Fractional mobility score
Time (minutes)
10 mM Nic
Nic + 312.5 μM OxoM
Nic + 1.25 mM OxoM
Nic + 2.5 mM OxoM
Nic + 5.0 mM OxoM
E
Fractional mobility score
Time (minutes)
N2 Nic + oxoM
gar-1 Nic + oxoM
gar-2 Nic + oxoM
gar-3 Nic + oxoM
F
Fractional mobility score
Time (minutes)
5mM Ald
10 mM oxoM
5mM Ald + 10 mM oxoM

Figure 6

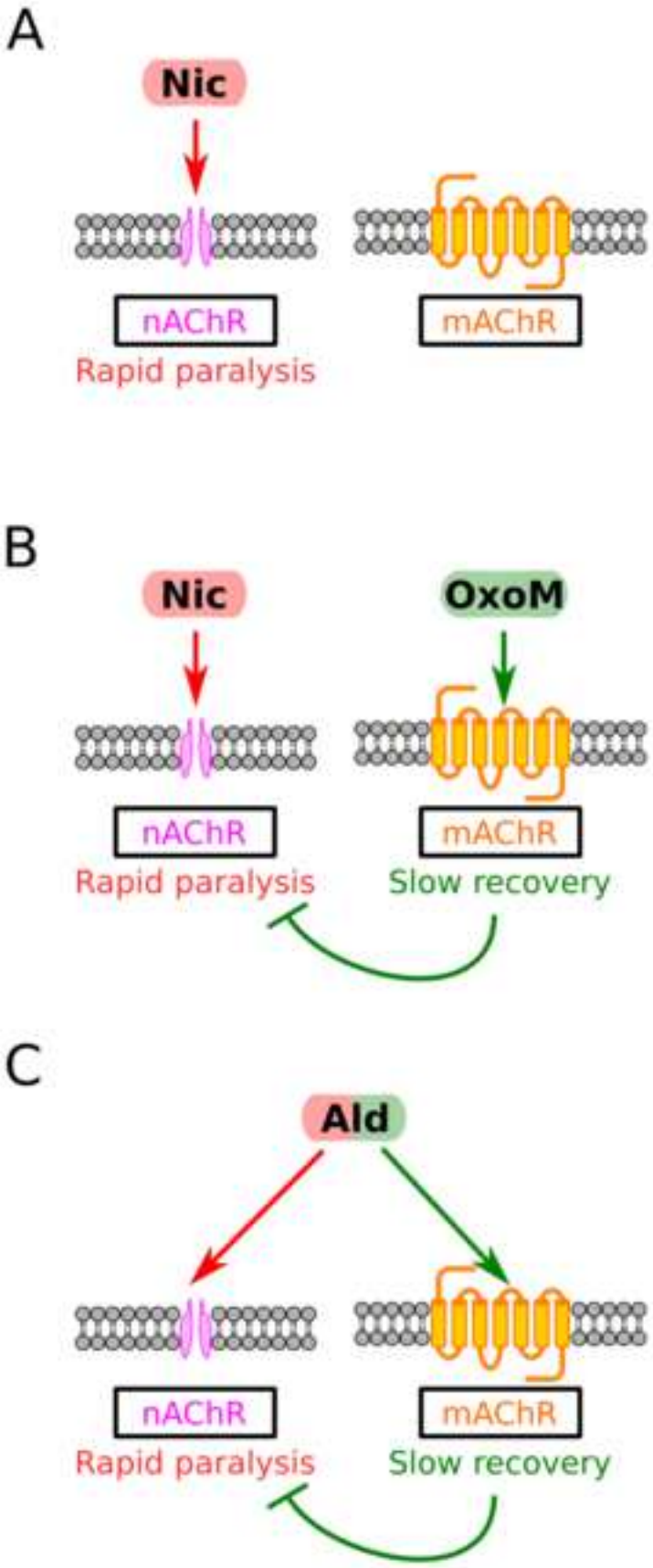
A
Nic
nAChR
Rapid paralysis
mAChR
B
Nic
OxoM
nAChR
Rapid paralysis
mAChR
Slow recovery
C
Ald
nAChR
Rapid paralysis
mAChR
Slow recovery

Click here to download Figure fig7.tif

Figure 7

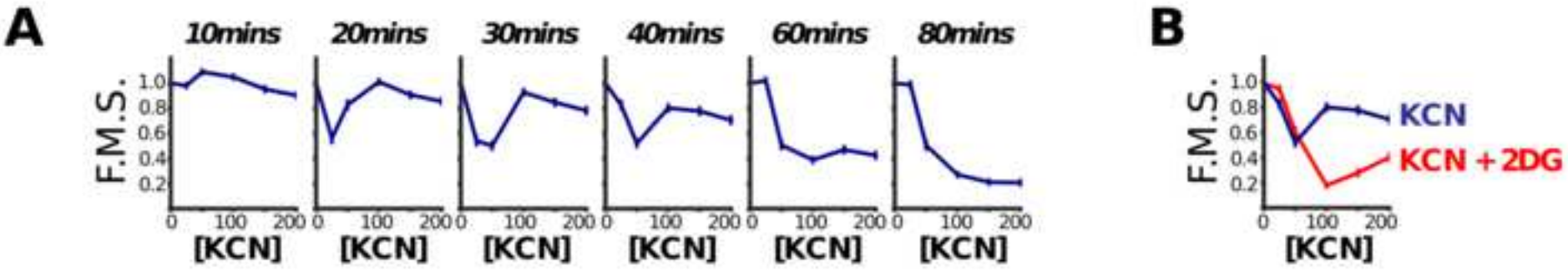

Click here to download Figure fig8.tif

Figure 8

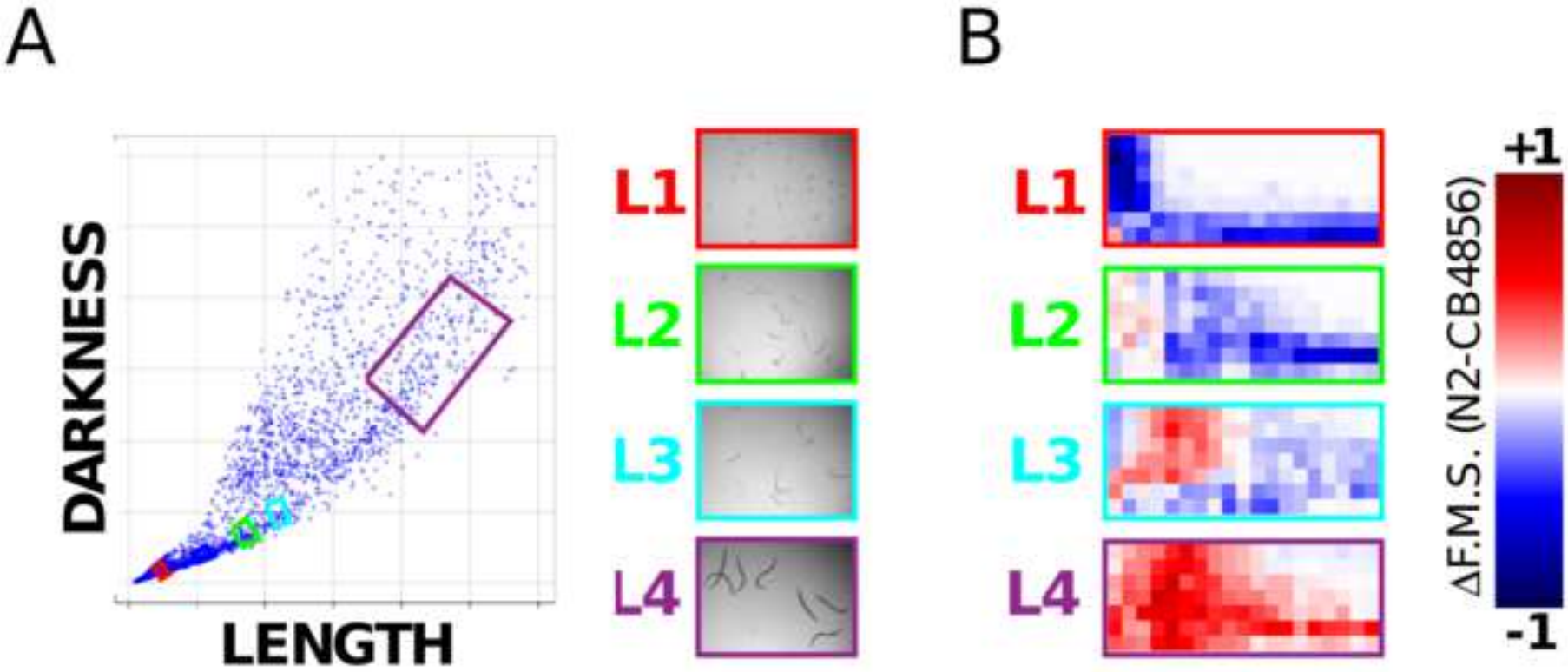

Click here to download Figure figS1.tif

Supplementary Figure 1

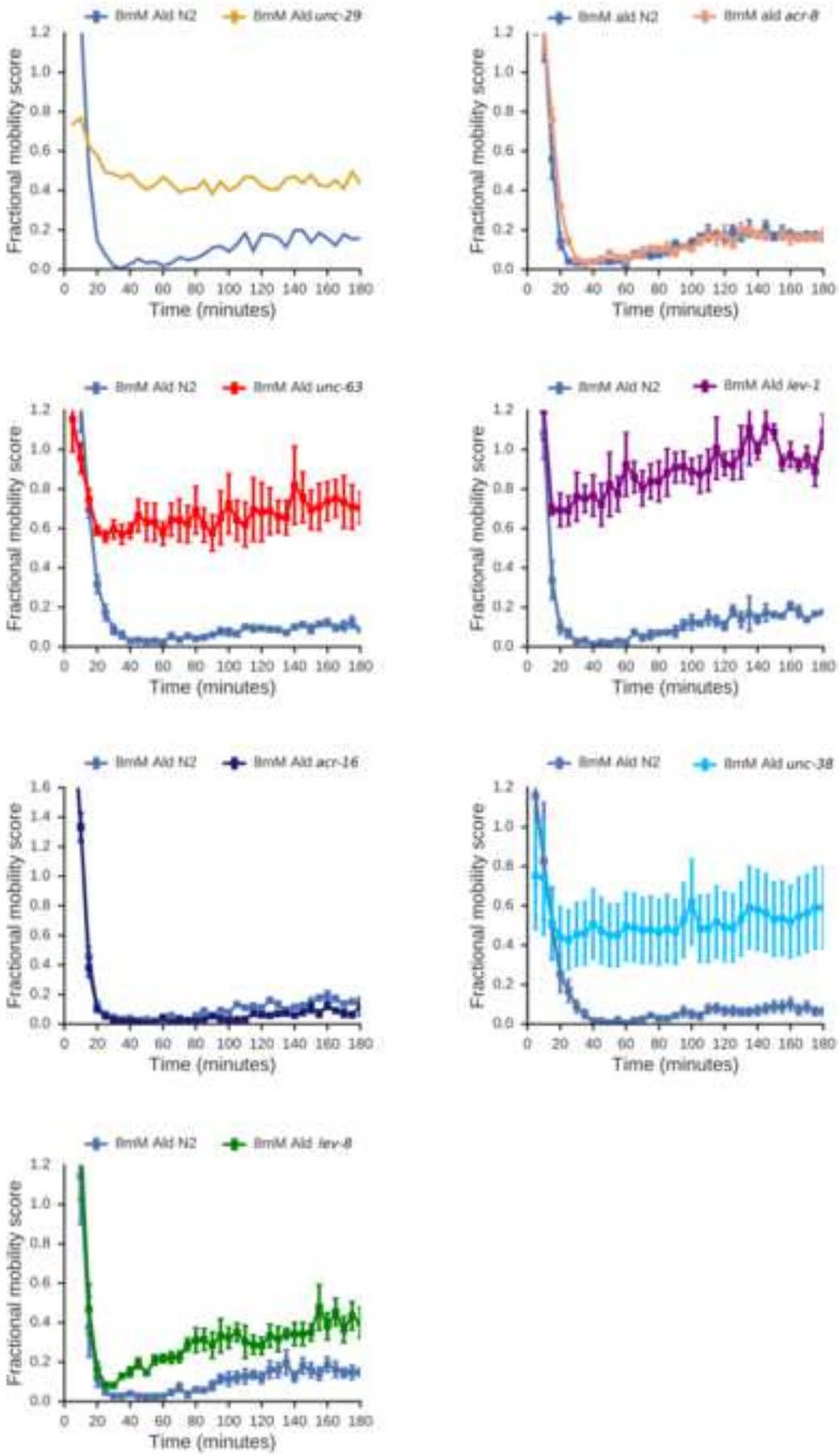

Click here to download Figure figS2.tif

Supplementary Figure 2

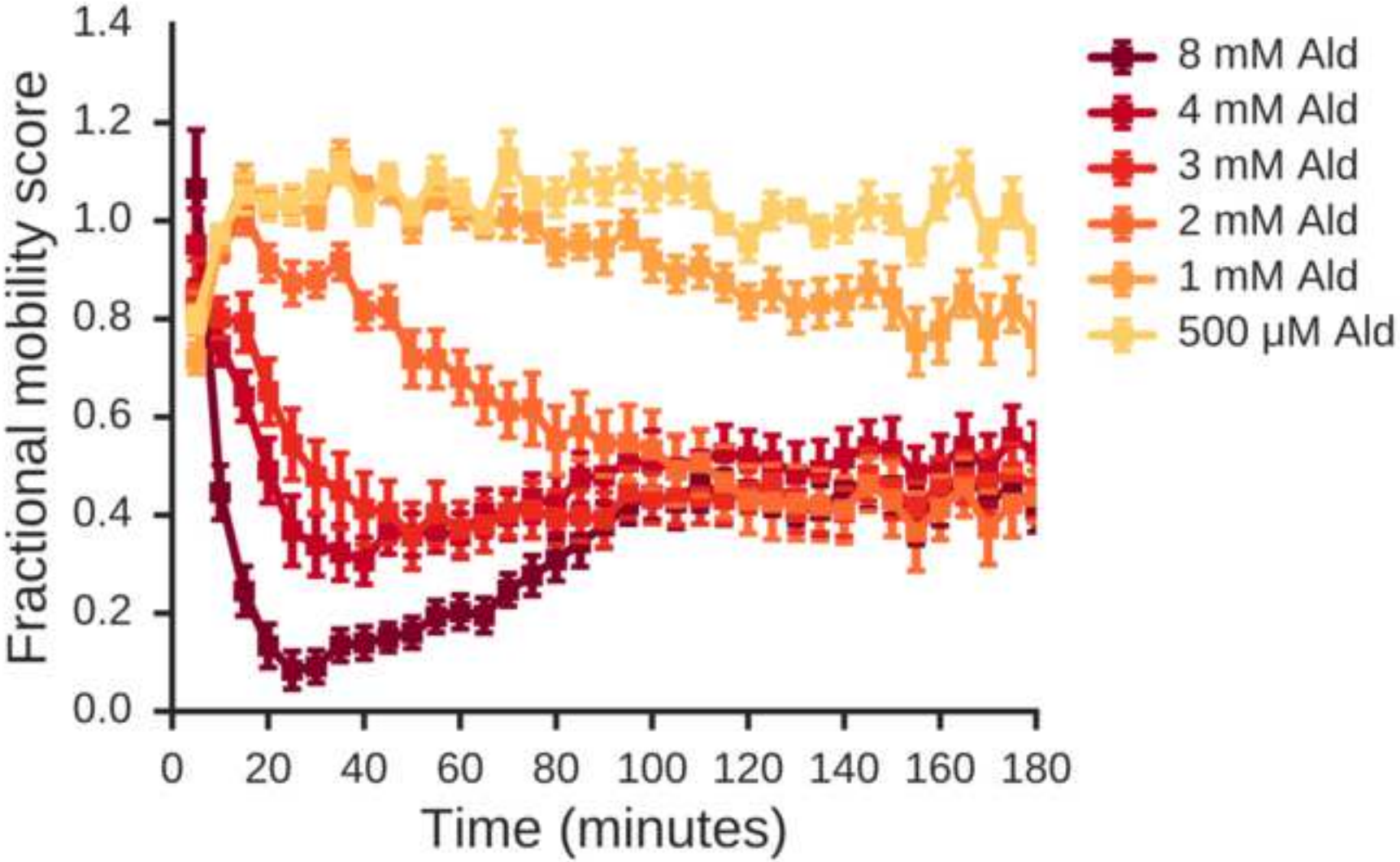

Click here to download Figure figS3.tif
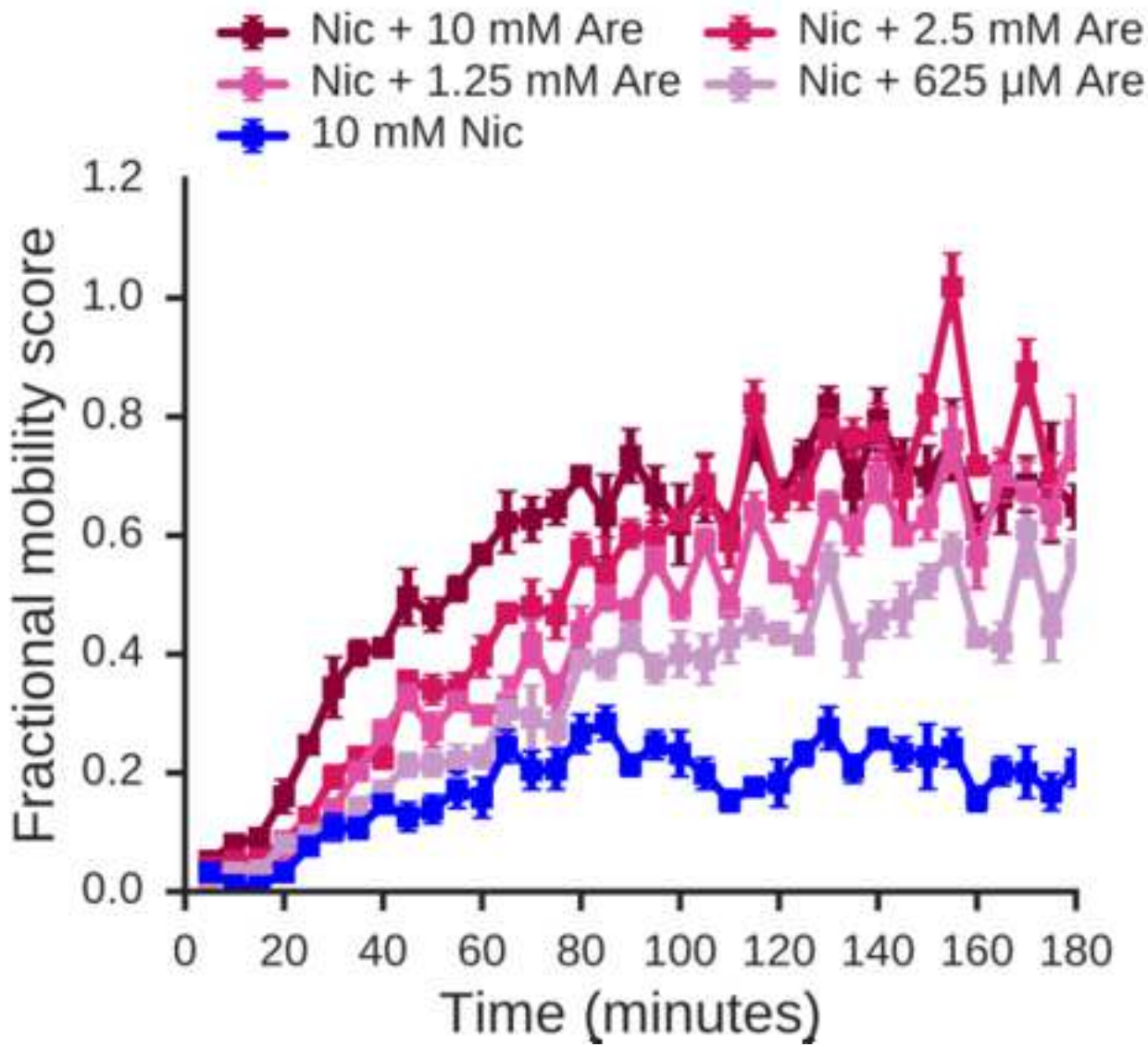
Supplementary Figure 3